IMSurReal: IMS at the Surface Realization Shared Task 2019

Xiang Yu, Agnieszka Falenska, Marina Haid, Ngoc Thang Vu, Jonas Kuhn
Institut für Maschinelle Sprachverarbeitung
Universität Stuttgart, Germany
firstname.lastname@ims.uni-stuttgart.de

Abstract

We introduce the IMS contribution to the Surface Realization Shared Task 2019. Our submission achieves the state-of-the-art performance without using any external resources. The system takes a pipeline approach consisting of five steps: linearization, completion, inflection, contraction, and detokenization. We compare the performance of our linearization algorithm with two external baselines and report results for each step in the pipeline. Furthermore, we perform detailed error analysis revealing correlation between word order freedom and difficulty of the linearization task.

1 Introduction

This paper presents our submission to the Surface Realization Shared Task 2019 (Mille et al., 2019). We participate in both shallow and deep track of the shared task, where the shallow track requires the recovery of the linear order and inflection of a dependency tree, and the deep track additionally requires the completion of function words.

We approach both tasks with very similar pipelines, consisting of linearizing the unordered dependency trees, completing function words (for the deep track only), inflecting lemmata to word forms, and contracting several words as one token, and finally detokenizing to obtain the natural written text. We use machine learning models for the first four steps and a rule-based off-the-shelf detokenizer for the final step.

In the evaluation on the tokenized text, our system achieves the highest BLEU scores for each individual treebank in both tracks, with an average of 79.97 for the shallow track and 51.41 for the deep track. In the human evaluation on four languages, we also rank the first in terms of readability and adequacy.

2 Surface Realization System

Our system takes a pipeline approach, which consists of up to five steps to produce the final detokenized text. The steps are: linearization (§2.2), completion (§2.3), inflection (§2.4), contraction (§2.5), and detokenization (§2.6), among which completion is used only in the deep track. All the steps except for the rule-based detokenization use the same Tree-LSTM encoder architecture (§2.1). As the multi-task style training hurt performance in the preliminary experiments, all the steps are trained separately.

Since the submission is mostly based on our system described in Yu et al. (2019b), here we mainly focus on the changes introduced for this shared task, and we refer the reader to Yu et al. (2019b) for more details, especially on the explanation and ablation experiments of the Tree-LSTM encoder and the linearization decoder.

2.1 Tree-LSTM Encoder

Representation of each token in the tree is based on its lemma, UPOS, morphological features, and dependency label. We use embeddings for the lemma, UPOS and dependency label, and employ an LSTM to process the list of morphological features.[1] We then concatenate all of the obtained vectors as the representation of each token ($\mathbf{v}^\circ$).

The representation is further processed by a bidirectional Tree-LSTM to encode the tree structure information. The encoder is generally the same as described in Yu et al. (2019b), consisting of two passes of information: a bottom-up pass followed by a top-down pass. In the bottom-up pass, we use a Tree-LSTM (Zhou et al., 2016) to compose the bottom-up vector of the head from the vectors of the dependents, attended by the

[1] There could be better treatment of the morphological features, since they are not sequences in nature.

token-level vector of the head, denoted as $\mathbf{v}^{\uparrow}$. The bottom-up vectors are then fed into a sequential LSTM for the top-down pass from the root to each leaf token, so that every token has access to all the descendants of all its ancestors, namely all tokens in the tree. The output vector is denoted as $\mathbf{v}^{\downarrow}$.

For linearization, we use the concatenation of $\mathbf{v}^{\uparrow}$ and $\mathbf{v}^{\downarrow}$ as the representation of each token. For the other tasks, where the sequence is already determined, we additionally use a sequential bidirectional LSTM to encode the sequence, with the tree-based vectors as input.

2.2 Linearization

The linearization algorithm is the same as in Yu et al. (2019b), which is in turn based on the linearizer described by Bohnet et al. (2010). The algorithm takes an *divide-and-conquer* strategy, which orders each subtree (a head and its dependents) individually, and then combines them into a fully linearized tree.[2]

The main improvement of our algorithm to Bohnet et al. (2010) is that instead of ordering the subtrees from left to right, we start from the head (thus called the head-first decoder), and add the dependents on both sides of the head incrementally. We also train a left-to-right and a right-to-left decoders to form an ensemble with a shared encoder, which is shown in Yu et al. (2019b) to achieve the best performance.

We use beam search to find the best linearization order of each subtree, where the best N partial hypotheses are kept to expand at each step. For the head-first decoder, we use two LSTMs to track the left and right expansion of the sequence (only one LSTM is needed for the left-to-right or right-to-left expansion), and the score of the sequence is calculated from the concatenation of the two LSTM states followed by an MLP.

Note that in the shared task some tokens are provided with information about the relative word order to its head.[3] We use these constraints in our decoder so that the hypotheses violating the constraints are ignored. Preliminary experiments showed that disregarding this word order information would decrease the BLEU score by 2-3 points.

2.3 Completion

The completion model for the deep track takes the output of the linearization model as input and insert function words into the linearized subtrees.

Similarly to the linearization algorithm, we also use a head-first strategy to complete each subtree. We use two pairs of LSTMs to encode the sequence: a pair of forward and backward LSTMs for the left dependents, and a pair for the right dependents, where "forward" means from the head to the end and "backward" means from the end towards the head. Since the two pairs are symmetrical, we only describe the decoding process to the right side of the head.

We use a pointer to indicate the current token, which initially points to the head. We use the backward LSTM to encode the upcoming sequence of linearized tokens, and the forward LSTM to encode the already processed tokens up to the pointer (which includes both the previously linearized tokens and the newly generated tokens).

At each decoding step, we concatenate the forward LSTM output of the current pointed token and the backward LSTM output of the next token, and calculate a softmax distribution of all possible function words, as well as a special symbol $\Rightarrow$, which moves the pointer to the next token. If a new token is generated, the pointer will point to the new token. If $\Rightarrow$ is predicted and the pointer already reached the last token in the sequence, then the completion process is terminated.

Figure 1 illustrate an example of the completion process to the right side of the head, where the linearized tokens are [h, $\mathrm{d}^{(+1)}$, $\mathrm{d}^{(+2)}$, \$], h is the head, $\mathrm{d}^{(+1)}$ and $\mathrm{d}^{(+2)}$ are right dependents, and \$ indicates the end of the subtree. In step (1) the symbol $\Rightarrow$ is predicted, therefore we move the pointer from the h to $\mathrm{d}^{(+1)}$; in step (2) a new token f_1 is created and attached to $\mathrm{d}^{(+1)}$; in step (3) another token f_2 is created and attached to f_1; in step (4) the pointer is moved to $\mathrm{d}^{(+2)}$; in step (5) the pointer is moved again to \$, which terminates the process and outputs the sequence [h, $\mathrm{d}^{(+1)}$, f_1, f_2, $\mathrm{d}^{(+2)}$].

The left and right completion processes are independent of each other, since both forward LSTMs are only aware of the initial linearized tokens on both sides but not the newly generated tokens. We tried several variations in the prelimi-

[2]This algorithm can only create projective trees. An method to bypass the projective constraints is described in Bohnet et al. (2012). However, we did not use this method and only produce projective trees due to limited time.

[3]The information are encoded in the morphological features, such as `lin=+2`, which means this token must appear after the token with the feature `lin=+1` after the head. They are provided for the cases that do not have a unique correct order, e.g., punctuation or coordinating conjunction.

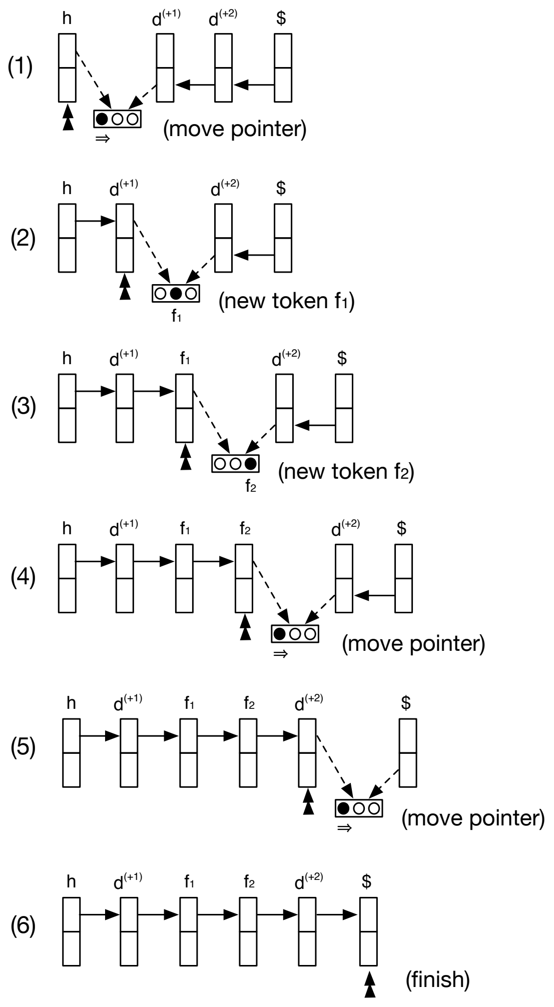

Figure 1: An example of the completion process to the right side, where the right arrows illustrate the forward LSTM, and the left arrows the backward LSTM.

nary experiments, including joint linearization and completion, interleaving the left and right completion processes, and beam-search for completion. All approaches yielded lower performance than the described method.[4] However, we note that the completion step seems to have the most potential to benefit from external language models. We observe that many generated function words are syntactically correct but semantically implausible, and the language models are generally good at capturing semantic coherence. We plan to incorporate language models in the future work.

[4]Admittedly, most of the experiments are rather brief, more careful design and thorough experiments might lead to different results.

2.4 Inflection

The inflection model is the same as in Yu et al. (2019b). It generates a sequence of edit operations that modifies the lemma into the inflected word form. The model takes the characters in the lemma as input and encodes through a bidirectional LSTM. A binary feature is concatenated to the vector of each character which functions as a pointer to indicate the input character currently to be processed. At each step, the decoder attends to the input vectors and predicts an output, which could be a symbol ✓ to copy the current input character, a symbol ✗ to ignore the current input character, or a character from the alphabet to generate a new one. When ✓ or ✗ is predicted, the input pointer will move one step forward, while if a character is generated, the input pointer does not move.

The ground truth of such sequence is calculated from the Levenshtein edit operations between the lemma and the word form, where only insertion and deletion is allowed (no substitution).

Our model is in a way similar to the hard monotonic attention in Aharoni and Goldberg (2017), but we use a much simpler source-target alignment (Levenshtein edit operations), and we use copy as an edit operation to avoid completion errors while they do not. Furthermore, our edit operations are associated with the moving of the pointer, while they treat moving the pointer as an atomic operation, which lead to longer prediction sequences. Generally, our model performs on a par with theirs, see the comparison in Yu et al. (2019b).

2.5 Contraction

In Yu et al. (2019b) we described a rule-based contraction method by constructing an automaton from the training data, which works reasonably well for most of the languages where the contraction is trivial. However, it works rather poorly for Arabic since the contraction is not just among closed class function words but also content words, so that the coverage of the rules is very small. It is also problematic for the verb-pronoun contraction in Spanish and Portuguese although they are much less frequent.

We therefore implement a character-based contraction model to alleviate this problem. The model works in two steps. First it predicts BIO tags to identify the groups of consecutive words that need to be contracted. Then it concatenates the group as a character sequence and predicts the contracted word form as output. We use a simple Seq2Seq model for the contraction due to limited time, although an edit based model similar to the one for inflection might yield better results.

2.6 Detokenization

The detokenization step is the same as described in Yu et al. (2019b), namely a rule-based tool MosesDetokenizer.[5] After the submission we realized that the tool removes all empty spaces in Korean texts, similar to Chinese and Japanese. However, Korean actually uses empty spaces to separate words, thus we expect lower score in the human evaluation for this language.

2.7 Discussion on Pipeline Order

In our pipeline, we choose the order of linearization, completion, and finally inflection. Our rationale for such order is as follows: (1) the inflection in some cases depends on the linearized sequence of lemmata, e.g., the English determiner "a/an" depends on whether the following noun begins with an vowel, therefore inflection is the last of the three steps; (2) the search-based linearization model is more reliable than the greedy completion model, therefore we first perform linearization to reduce error propagation.

However, this choice is only based on our intuition, and one could come up with arguments for the alternative orders. For example, since inflection is the easiest and most accurate task, performing it first might further reduce error propagation. Further experiments are needed to determine the best order in the pipeline. Alternatively, a carefully designed joint prediction might address the error propagation problem, however, our initial attempts did not yield positive outcome.

2.8 Implementation Details

All the neural models are implemented with the DyNet library(Neubig et al., 2017), and the full system is available at the first author's website.[6] We use the embedding size of 64 for lemma and character, and 32 for UPOS, XPOS, morphological features, and dependency labels. The output dimension of the bottom-up and top-down encoder LSTMs, as well as all the decoder LSTMs, are equal to the input dimension. The beam size for the linearization is 32. We train the model up to 100000 steps without batching using the Adam optimizer (Kingma and Ba, 2014), test on the development set every 2000 steps, and stop training if there is no improvement 10 times in a row. All the hyperparameters are only minimally tuned to balance speed and performance, and kept the same for all languages.

The training and prediction of each treebank are run on single CPU cores. Depending on the treebank size, the training time of linearization models typically ranges from 1 to 10 hours. The completion, inflection, and contraction models are much faster, mostly under 1 hour, since they are all greedy models.

The prediction speed is around 10 sentence per second, which is not very fast, however, we did not perform any optimization toward speed (e.g. mini-batch, multi-processing, etc.) due to the experimental nature of our work.

3 Data

The training and test data in the shared task is based on Universal Dependencies (Nivre et al., 2016), see the overview paper for the details.

We do not use any external resources for our system, except that we concatenate the training treebanks for some languages (see Table 3 and 4). However, not all treebanks benefits from the concatenation, since the idiosyncrasies in the UD treebanks can hurt the performance as noted in Björkelund et al. (2017), where the concatenation of multiple UD treebanks also hurts parsing performance.

Evaluation in the shared task is also performed on out-of-domain datasets, namely the automatically parsed trees from some in-domain treebanks and the unseen PUD treebanks. We use the same model for the automatically parsed trees as for the gold ones, and use the model trained on concatenated treebanks for the PUD test data.

Some treebanks have XPOS tag set quite different from the UPOS, which could be useful as complementary information. We used XPOS as features when the tag set size is at least twice as large as the UPOS set size and smaller than 500 (to avoid sparsity). In fact, the XPOS tags in some treebanks could be decomposed as morphological features, e.g., Arabic, Indonesian, Korean. In

[5]https://pypi.org/project/mosestokenizer/

[6]https://www.ims.uni-stuttgart.de/institut/mitarbeiter/xiangyu/

the submission, we only choose to decompose the XPOS for Korean because it can be easily split by the "+" delimiter and both Korean treebanks do not have morphological features otherwise. We also use the real stems in the Korean treebanks by removing the suffixes after the "+" delimiter in the lemmata, in order to reduce the out-of-vocabulary problem, and the information on the suffixes are well preserved in the morphological features derived from the XPOS.

Finally, since contraction appears only in Arabic, Spanish, French and Portuguese, we therefore only train contraction models for these languages.

4 Evaluation

The automatic evaluation results of our submission to the shared task are shown in Table 1 and Table 2 for the shallow and deep tracks, respectively. The first three columns contain the BLEU, DIST, and NIST scores of our system, and the fourth column is the difference of BLEU scores between our system and the best system among other participants for each treebank.

Our system achieve the best performance for all treebanks in both tracks. Comparing to the best scores of other teams, the differences range from single digits for the English treebanks to about 20 points for most other treebanks and 38 points for Arabic. In the out-of-domain scenario, our system performs very stable in most of the cases. However, comparing to the English and Japanese PUD treebanks, the performance drop on Russian PUD treebank is quite notable. Our conjecture is that the annotation of the PUD treebank is much closer to the GSD treebank than the SynTagRus treebank. Since we use both treebanks for training, the much larger size of SynTagRus might have dominated the training.

In the human evaluation (see Mille et al. (2019) for details), we also rank the first in all four languages (English, Russian, Chinese and Spanish) both for readability and adequacy.

5 Analysis

5.1 Pipeline Performance

Table 3 and 4 show the results on the development sets of the in-domain treebanks for the shallow track and deep track, respectively. We also provide the linearization baselines by Puduppully

	BLEU	NIST	DIST	Δ_{BLEU}
ar_padt	64.90	12.22	73.71	38.50
en_ewt	82.98	13.61	86.72	3.29
en_gum	83.84	12.69	83.49	1.45
en_lines	81.00	12.71	82.21	5.51
en_partut	87.25	11.01	85.68	8.27
es_ancora	83.70	14.69	79.82	7.23
es_gsd	82.98	12.77	79.45	12.83
fr_gsd	84.00	12.45	84.15	23.85
fr_partut	83.38	10.36	82.32	17.37
fr_sequoia	85.01	12.53	85.13	22.22
hi_hdtb	80.56	13.07	79.07	11.33
id_gsd	85.34	12.83	83.92	21.63
ja_gsd	87.69	12.42	87.17	24.10
ko_gsd	74.19	12.27	80.95	28.11
ko_kaist	73.93	13.00	78.69	26.70
pt_bosque	77.75	12.15	79.80	25.06
pt_gsd	75.93	13.07	79.33	23.43
ru_gsd	71.23	12.15	73.04	16.14
ru_syntagrus	76.95	15.08	78.66	16.96
zh_gsd	83.85	12.78	83.18	15.31
en_pud	86.61	13.47	87.00	2.54
ja_pud	86.64	13.02	84.04	20.12
ru_pud	58.38	10.91	77.12	6.01
en_ewt-pred	81.80	13.46	85.35	4.59
en_pud-pred	82.60	13.26	86.18	1.94
es_ancora-pred	83.31	14.61	81.14	6.03
hi_hdtb-pred	80.19	13.05	78.88	10.27
ko_kaist-pred	74.27	13.02	79.12	27.55
pt_bosque-pred	78.97	12.14	81.56	25.33
AVG	79.97	12.79	81.62	15.64

Table 1: Automatic Evaluation Results of the shallow track (T1) and the BLEU difference with the best system among other participants for each treebank.

	BLEU	NIST	DIST	Δ_{BLEU}
en_ewt	54.75	11.79	76.30	25.17
en_gum	52.45	11.04	73.07	25.85
en_lines	47.29	10.63	71.93	18.21
en_partut	45.89	9.03	67.45	17.04
es_ancora	53.13	12.38	68.58	16.15
es_gsd	51.17	10.82	68.85	16.52
fr_gsd	53.62	10.79	68.82	28.02
fr_partut	46.95	8.27	68.99	18.76
fr_sequoia	57.41	11.00	72.06	28.85
en_pud	51.01	11.45	72.31	24.45
en_ewt-pred	53.54	11.55	74.99	24.91
en_pud-pred	47.60	11.08	71.65	21.83
es_ancora-pred	53.54	12.36	70.02	16.13
AVG	51.41	10.94	71.16	21.68

Table 2: Automatic Evaluation Results of the deep track (T2) and the BLEU difference with the best system among other participants for each treebank.

	P16	B10	lin*	lin	inf	con	final
ar_padt	77.73	82.69	84.24	87.27	95.63	91.59	68.58
en_ewt	79.10	82.71	85.11	88.01	98.47		84.50
en_gum	74.03	82.36	83.69	87.29	98.23		84.35
en_lines(+)	69.47	75.69	78.39	82.40	97.86		79.05
en_partut	71.45	80.11	86.38	89.14	97.94		86.25
es_ancora	74.57	81.61	83.47	85.33	99.51	99.86	84.43
es_gsd(+)	78.28	82.32	83.53	86.18	99.18	99.09	84.04
fr_gsd(+)	82.99	85.26	87.02	89.74	98.63	99.47	86.98
fr_partut	71.46	83.92	87.07	90.08	96.95	99.44	84.17
fr_sequoia	74.16	83.66	87.09	90.39	98.20	99.58	86.51
hi_hdtb	79.83	82.03	82.79	85.25	98.11		81.62
id_gsd	74.68	78.27	81.23	86.05	99.51		84.62
ja_gsd	86.20	89.08	90.41	92.55	98.69		89.49
ko_gsd(+)	67.55	69.48	76.05	79.66	96.74		74.25
ko_kaist(+)	76.98	77.47	78.73	80.01	97.32		76.04
pt_bosque	76.97	80.30	82.48	84.35	99.31	98.23	80.75
pt_gsd	83.19	86.53	87.17	89.24	94.99	99.84	76.89
ru_gsd	68.32	74.04	74.64	79.09	95.98		73.66
ru_syntagrus(+)	73.58	77.01	78.52	80.97	97.84		76.28
zh_gsd	68.92	75.60	81.22	84.10	100.00		83.34
AVG	75.47	80.51	82.96	85.86	97.95		81.29

Table 3: Development results in the shallow track, including the linearization baselines.

	lin	comp	inf	con	final
en_ewt	80.17	67.70	97.98		55.27
en_gum(+)	76.14	61.44	97.72		50.53
en_lines(+)	76.63	60.47	97.16		47.17
en_partut(+)	73.80	60.63	97.63		44.59
es_ancora	77.88	66.95	98.25	99.85	53.57
es_gsd	77.98	69.72	97.85	99.71	53.81
fr_gsd(+)	81.36	73.20	97.63	99.26	57.46
fr_partut(+)	75.36	65.94	94.64	98.39	48.17
fr_sequoia(+)	80.03	73.01	97.04	99.60	58.27
AVG	77.40	66.42	97.24		51.70

Table 4: Development results in the deep track.

et al. (2016) (P16) and Bohnet et al. (2010) (B10).[7] The columns show different evaluation metrics on different targets. Except for the final column, each one evaluates on only one step assuming all previous steps are gold.

In Table 3, columns 1-4 are the BLEU scores of linearization evaluated on the lemmata, column 5 is the accuracy of inflection, column 6 is BLEU score on the contracted word form (empty cells means contraction is not applied), column 7 is the final BLEU score of the full pipeline. The column lin* shows the models trained on single treebanks and without using the word order information, which allows a fair comparison to the two baselines. The models marked with + are trained with concatenated treebanks for the submission, which performs slightly better than the single treebank, typically by 0.5-1 BLEU points. For each treebank, we either use the concatenated treebank to train all steps in the pipeline or use the single treebank for all steps, depending on the final BLEU score on the development set.

In Table 4, column 1 is the BLEU score on the lemmata of the given content words, columns 2 is the BLEU score on the lemmata including generated tokens, column 3 is the accuracy on word forms, column 4 is the BLEU score of contracted word forms, and column 5 is the BLEU score of the full pipeline. Similar to Table 3, the models marked with + are trained with concatenated treebanks.

In the shallow track, our linearization model outperforms the best baseline (Bohnet et al., 2010) by 2.5 BLEU points on average. The inclusion of word order information (and treebank concatenation to a much smaller extent) brings about 3 additional points. For the deep track, the BLEU score of linearization is much higher than completion, which motivates our decision to perform linearization before completion.

5.2 Word Order Preferences

In this section we analyze the relation between word order preferences of each language and the errors made by the linearizer,[8] characterized by

[7]We run the two baseline systems *as is*, where we only convert the input format to ensure all systems are using the same information and keep their default options.

[8]Note that an "error" is counted when the predicted order is different from the original order in the reference, however,

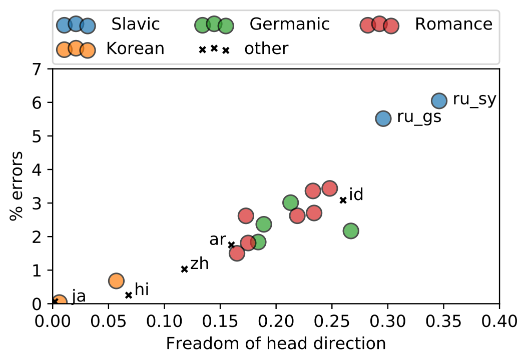

(a) Head direction freedom vs. errors.

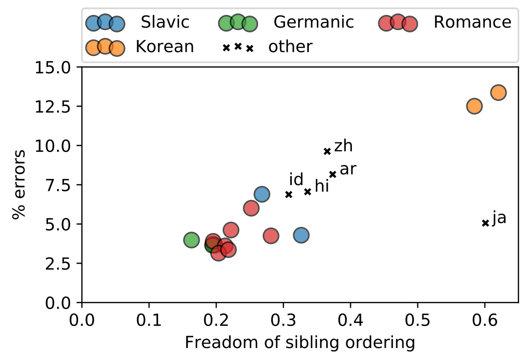

(b) Sibling ordering freedom vs. errors.

Figure 2: The correlation of word order freedom and linearization errors. Different language families are marked with different colors.

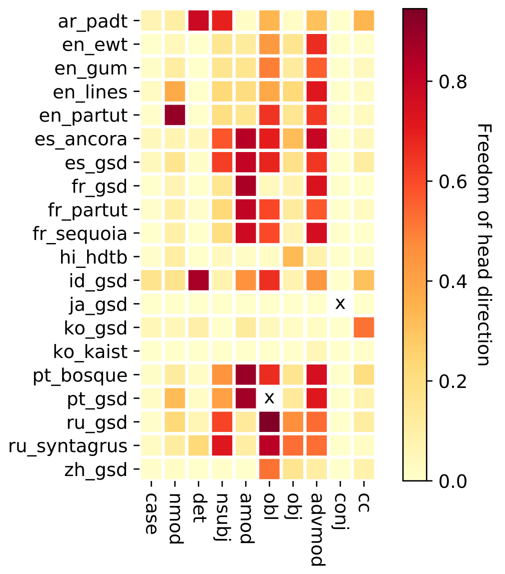

(a) Head direction freedom of each dependency relations in each training set.

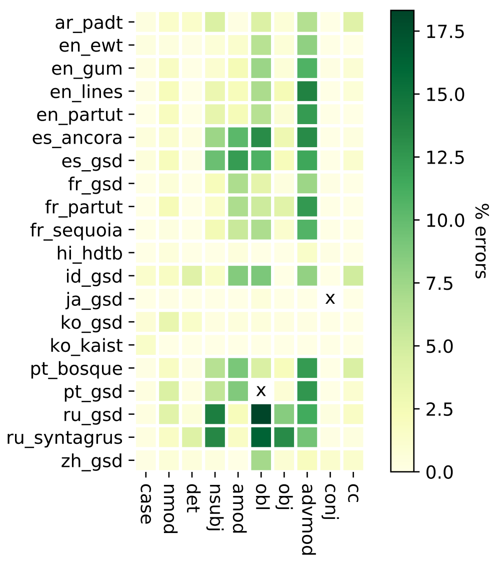

(b) Head direction errors of each dependency relations in each development set.

Figure 3: Detailed visualization of head direction freedom vs. linearization errors of the 10 most frequent dependency relations in each treebank, where "x" means no such relation in the treebank.

two types of word order preferences as defined in Yu et al. (2019a):

head direction – whether the dependent appears to the left or the right side of the head;

sibling order – the order of a pair of dependents on the same side of the head.

We then define the freedom of these two types of word order preferences, namely the entropy of the word order of each dependency relation, which is described in details in Yu et al. (2019a)[9]. In both types of word orders, higher freedom means less constraints on the word order.

We also calculate the error rate of the linearizer by the dependency relations:

head direction – whether the dependent appears on the correct side of the head;

sibling order – whether a pair of dependents on the same side of the head has the correct order.

Figure 2 shows the correlation of freedom and linearization errors of the two types of word orders. For both head direction (Figure 2a) and sibling ordering (Figure 2b), we can observe quite strong correlation of the freedom and linearization errors. For the head direction, both Russian treebanks have the highest freedom, and the linearizer

this does not mean that the predicted one is incorrect. The variation of word order in natural languages can not be trivially evaluated by the single reference BLEU score, human judgement is thus needed for a more accurate evaluation.

[9]Here we only use the dependency relations to characterize the word orders for simplicity of visualization, while Yu et al. (2019a) additionally use the UPOS tag, which is more fine-grained.

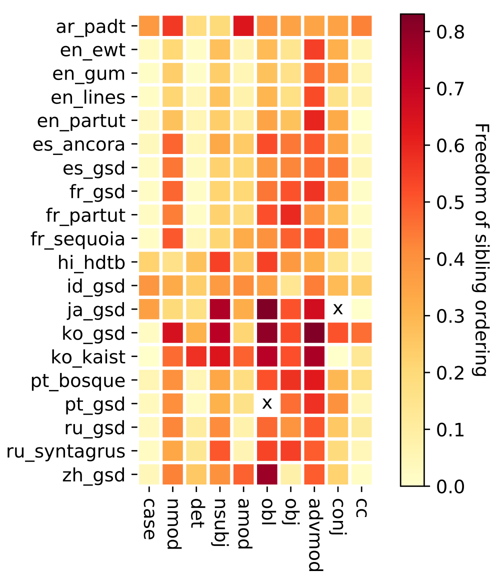

(a) Sibling ordering freedom of each dependency relations in each training set.

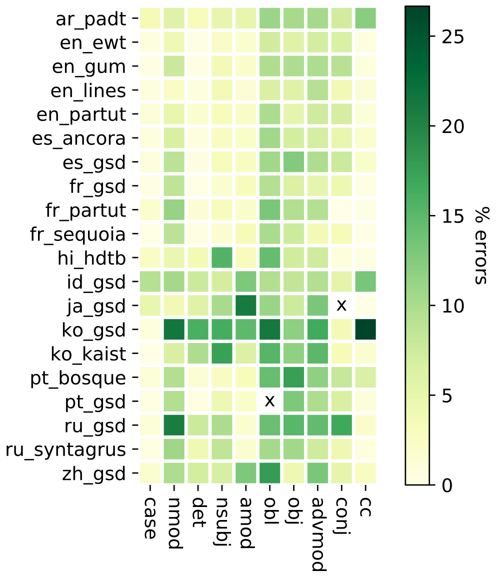

(b) Sibling ordering errors of each dependency relations in each development set.

Figure 4: Detailed visualization of sibling ordering freedom vs. linearization errors of the 10 most frequent dependency relations in each treebank, where “x” means no such relation in the treebank.

also makes the most errors. Verb final languages such as Korean, Japanese and Hindi, on the contrary, have the lowest freedom and the least errors. For the sibling ordering, both Korean treebanks have the highest freedom and linearization error rate. However, there are no treebanks with very low freedom or error rate, which suggests that the ordering of arguments are generally less strict than the head direction in all languages.

We then look into the errors of our system in more details. We take ten most common dependency relations in all the treebanks (we map the language-specific relation subtypes to their general type, e.g., nmod:poss is mapped to nmod) and calculate their freedom and the linearization error rate. Figure 3 presents results for the head direction constraint, where the intensity patterns of the freedom and error rate align very well. Interestingly, the verb-final languages have very low freedom and error rate across almost all relations, not only verb arguments. For the most other languages, obl and advmod are difficult; amod is difficult for Romance languages; and nsubj is difficult for Russian.

Figure 4 shows the freedom and error rate for sibling ordering. The freedom of particular relations (Figure 4a) and their linearization errors (Figure 4b) also show quite similar patterns, although less clear than the head direction.

In particular, some relations with very high freedom do not have high error rate, e.g. many verb arguments in Japanese. This suggests that the lexicalized linearization model can capture more sophisticated word order information than the coarse word order preferences defined by the dependency relations.

6 Conclusion

We have presented our surface realization system, which performs both shallow and deep completion. The system achieves state-of-the-art results without any external data.

As future work, we plan to focus on improving the completion model, since it is currently the performance bottleneck of the deep generation task, which is a more realistic task for NLG applications. We also plan to incorporate ranking methods with and without external language models to further improve the linearization, since the described results suggest that there is room for improvement.

Acknowledgements

This work was in part supported by funding from the Ministry of Science, Research and the Arts of the State of Baden-Württemberg (MWK), within the CLARIN-D research project.

References

Roee Aharoni and Yoav Goldberg. 2017. Morphological Inflection Generation with Hard Monotonic Attention. In *Proceedings of the 55th Annual Meeting of the Association for Computational Linguistics (Volume 1: Long Papers)*, pages 2004–2015.

Anders Björkelund, Agnieszka Falenska, Xiang Yu, and Jonas Kuhn. 2017. IMS at the CoNLL 2017 UD Shared Task: CRFs and Perceptrons Meet Neural Networks. In *Proceedings of the CoNLL 2017 Shared Task: Multilingual Parsing from Raw Text to Universal Dependencies*, pages 40–51, Vancouver, Canada. Association for Computational Linguistics.

Bernd Bohnet, Anders Björkelund, Jonas Kuhn, Wolfgang Seeker, and Sina Zarrieß. 2012. Generating Non-Projective Word Order in Statistical Linearization. In *Proceedings of the 2012 Joint Conference on Empirical Methods in Natural Language Processing and Computational Natural Language Learning*, pages 928–939.

Bernd Bohnet, Leo Wanner, Simon Mille, and Alicia Burga. 2010. Broad Coverage Multilingual Deep Sentence Generation with a Stochastic Multi-Level Realizer. In *Proceedings of the 23rd International Conference on Computational Linguistics*, pages 98–106. Association for Computational Linguistics.

Diederik P. Kingma and Jimmy Ba. 2014. Adam: A Method for Stochastic Optimization.

Simon Mille, Anja Belz, Bernd Bohnet, Yvette Graham, and Leo Wanner. 2019. The Second Multilingual Surface Realisation Shared Task (SR'19): Overview and Evaluation Results. In *Proceedings of the 2nd Workshop on Multilingual Surface Realisation (MSR), 2019 Conference on Empirical Methods in Natural Language Processing (EMNLP)*, Hong Kong, China.

Graham Neubig, Chris Dyer, Yoav Goldberg, Austin Matthews, Waleed Ammar, Antonios Anastasopoulos, Miguel Ballesteros, David Chiang, Daniel Clothiaux, Trevor Cohn, et al. 2017. Dynet: The Dynamic Neural Network Toolkit. *arXiv preprint arXiv:1701.03980*.

Joakim Nivre, Marie-Catherine De Marneffe, Filip Ginter, Yoav Goldberg, Jan Hajic, Christopher D Manning, Ryan McDonald, Slav Petrov, Sampo Pyysalo, Natalia Silveira, et al. 2016. Universal Dependencies v1: A Multilingual Treebank Collection. In *Proceedings of the Tenth International Conference on Language Resources and Evaluation (LREC 2016)*, pages 1659–1666.

Ratish Puduppully, Yue Zhang, and Manish Shrivastava. 2016. Transition-based Syntactic Linearization with Lookahead Features. In *Proceedings of the 2016 Conference of the North American Chapter of the Association for Computational Linguistics: Human Language Technologies*, pages 488–493.

Xiang Yu, Agnieszka Falenska, and Jonas Kuhn. 2019a. Dependency Length Minimization vs. Word Order Constraints: An Empirical Study On 55 Treebanks. In *Proceedings of the First Workshop on Quantitative Syntax (Quasy, SyntaxFest 2019)*, pages 89–97, Paris, France. Association for Computational Linguistics.

Xiang Yu, Agnieszka Falenska, Ngoc Thang Vu, and Jonas Kuhn. 2019b. Head-first linearization with tree-structured representation. In *Proceedings of the 12th International Conference on Natural Language Generation*, Tokyo, Japan.

Yao Zhou, Cong Liu, and Yan Pan. 2016. Modelling Sentence Pairs with Tree-structured Attentive Encoder. In *Proceedings of COLING 2016, the 26th International Conference on Computational Linguistics: Technical Papers*, pages 2912–2922.